Ab Initio Molecular Dynamics Study of the Reaction between Th^+ and H_2O†

Jia Zhou and H. Bernhard Schlegel*

Department of Chemistry, Wayne State University, Detroit, Michigan 48202

Received: December 22, 2009; Revised Manuscript Received: February 11, 2010

The gas phase reaction of Th^+ with H_2O to produce $HThO^+ + H$ and $ThO^+ + H_2$ was investigated using density functional theory and coupled cluster methods. RRKM calculations of the branching ratio favor the H atomic elimination channel in disagreement with experiment. Ab initio classical trajectory calculations were carried out to obtain a better model of the molecular dynamics. The molecular dynamics simulations yield a branching ratio of ca. 80% for the H_2 elimination channel to 20% for the H atomic elimination channel in qualitative agreement with the observed ratio of 65% to 35%.

Introduction

Within the last decades, reactions of actinide cations with small molecules in the gas phase have attracted significant attention.[1−21] In these reactions, the distinctive electronic structures and chemical properties of the f-block elements can be studied in the absence of perturbing factors such as solvation or lattice neighbors. The actinides are the 5f homologues of the lanthanides, with the 5f valence orbitals being filled between Ac and Lr, but they are notably different from the lanthanides, in which the 4f electrons do not participate in bond formation. Potential contribution of the 5f electrons to the reactivity is of great interest, particularly for early actinides, because the 5f electrons are relatively high in energy and are spatially extended. Consequently, numerous studies have then been carried out on the reactions of actinide cations with small molecules both experimentally[1−17] and theoretically.[18−21] The experimental studies have already been comprehensively reviewed.[1−3] One of the techniques used in the study of the reactivity of actinides is laser ablation with prompt reaction and detection (LAPRD).[3] Gibson and Haire reported the reactions of Pa^+ and PaO^+ with neutral molecules, showing that Pa^+ is very reactive with the reagents as diverse as alkenes, ethylene oxide, and sulfur hexafluoride.[4] Further investigations by the same group also include the reactions of Es^+ with dimethyl ether, 1,2-ethanedithiol, and 1,2,3,4,5-pentamethylcyclopentadiene.[5,6] LAPRD studies have established a following ordering of reactivities: $Th^+ \geq Pa^+ \geq U^+ \approx Np^+ > Cm^+ \geq Pu^+ > Bk^+ > Am^+ \approx Cf^+ \geq Es^+$. Fourier transform ion cyclotron resonance mass spectrometry (FTICR/MS) has been used extensively to study actinide ion reactivity and can be used to measure reaction kinetics, which cannot be accomplished by LAPRD. Reactions of An^+ and AnO^+ (An = Th, U, Np, Pu, Am) with a number of oxidants were studied with the aid of FTICR/MS and reaction efficiencies were obtained.[7−9] Additional investigations examined the reactivity of dications,[10] and studied the activation of hydrocarbons.[11−14] Quadruple ion trap mass spectrometry (QIT/MS) has also been used to examine the reactivity of actinide ions, and the differences between QIT/MS and FTICR/MS were explored by Jackson et al.[15−17] in a study of the reactivity of Th^+, U^+, ThO^+, UO^+, and UO_2^+, with HCp*.

The experimental techniques discussed above unquestionably provide novel information on the gas phase reactivity of actinide ions. However, limitations do still exist in terms of detailed information about the reaction mechanisms. Therefore, theoretical studies can be particularly valuable in providing additional information. Uranium is one of the most well-studied actinides, and in particular, the reactions of $U^{+/2+}$ and $UO^{+/2+}$ with H_2O and N_2O were first investigated by density functional theory (DFT) to examine O−H and N−O bond activation by uranium ions.[18−20]

In addition to uranium and its oxides, thorium cations are able to activate the O−H bonds in water. Reactions of Th^+ and Th^{2+} with water have been detected by the FTICR/MS experiments, and the products included ThO^+ and $ThOH^+$.[8−10] Further analyses indicate that ThO^+ is the major product (branching ratio 65%) over $ThOH^+$ (branching ratio 35%) for Th^+,[8,9] whereas $ThOH^+$ dominates with a branching ratio of 90% for Th^{2+}.[10] Furthermore, the potential energy surfaces of Th^+ and Th^{2+} with water have been mapped by several DFT methods.[21]

The present work focuses on the dynamics of the reaction of Th^+ with water. A range of theoretical methods are used to obtain better estimates of the structure and thermodynamics. The dynamics of the reaction are investigated by means of ab initio molecular classical trajectory calculations.

Method

Three different levels of theory were used to optimize the geometries of the minima and the transition states on the potential energy surface of the dissociation of $ThOH_2^+$. First, the B3LYP,[22−24] PW91PW91,[25,26] TPSSTPSS,[27] BHandHLYP, and BMK[28] functionals were used, along with the Stuttgart relativistic effective core potential (SDD)[29] for Th (30 valence electrons), and the 6-311++G(d,p) basis set for O and H atoms (designated as SDD). These calculations were carried out using the Gaussian suite of programs.[30] Second, calculations employing the relativistic two-component zero-order regular approximation (ZORA) with both scalar relativistic (SR) and spin−orbit (SO) effects were performed with the ADF code.[31−33] The PW91 exchange correlation energy functional and the TZP basis set for Th (frozen core, 12 valence electrons) and the TZ2P basis set for H_2O (O 1s frozen) were used for geometry optimization and frequency calculations (designated as PW91/ZORA-SR and PW91/ZORA-SO). Finally, coupled cluster (CCSD(T))[34] calculations with the SDD basis for Th and

† Part of the "Klaus Ruedenberg Festschrift".

* Corresponding author. Tel: (313)577-2562. Fax: (313)577-8822. E-mail: hbs@chem.wayne.edu.

10.1021/jp912098w
Published on Web 02/23/2010

6-311++G(d,p) for O and H atoms were carried out using the MOLPRO package.[35]

Similar to G2(MP2)[36] and G3(MP2)[37] treatment, we estimated CCSD(T) energies for all the species with an even larger basis set (designated SDD+, SDD plus two additional g functions for Th atom and 6-311++G(3df,2p) for O and H atoms) by using a composite approach:

$$E(\text{est.CCSD(T)/SDD+}) = E(\text{CCSD(T)/SDD}) + (E(\text{MP2/SDD+}) - E(\text{MP2/SDD}) \quad (1)$$

Ab initio classical trajectories were computed at the PW91/SDD level of theory using a Hessian-based predictor-corrector method[38,39] with the Gaussian suite of program. A predictor step is taken on the quadratic surface obtained from the energy, gradient and Hessian from the beginning point. A fifth-order polynomial is then fitted to the energies, gradients, and Hessians at the beginning and end points of the predictor step, and the Bulirsch−Stoer algorithm[40] is used to take a corrector step on this fitted surface with the angular forces projected out. The Hessians are updated for five steps before being recalculated analytically. The trajectories were terminated when the centers of mass of the fragments were 10 bohr apart and the gradient between the fragments was less than 1×10^{-5} hartree/bohr. A step size of 0.25 amu$^{1/2}$ bohr was used for integrating the trajectories. The energy was conserved to better than 1×10^{-5} hartree and the angular momentum was conserved to 1×10^{-8} $\hbar$.

Trajectories were initiated at the transition state for the Th^+ insertion into the O−H bond of water. A microcanonical ensemble of initial states was constructed using the quasi-classical normal mode sampling.[41,42] Since **TS1** is estimated to be at least 20 kcal/mol below the $Th^+ + H_2O$ reactants,[21] a total energy of 20 kcal/mol above the zero point energy of the transition state was distributed among the five vibrational modes and translation along the transition vector toward the product. The total angular momentum was set to zero (corresponding to a rotationally cold distribution), and the phases of the vibrational modes were chosen randomly. The momentum and displacement were scaled so that the desired total energy was the sum of the vibrational kinetic energy and the potential energy obtained from the ab initio surface. The initial conditions are similar to those used in previous trajectory calculations.[43,44] A total of 200 trajectories were integrated for up to 400 fs starting from the transition state. Of these, 36 were unsuccessful because of SCF convergence failure or lack of conservation of energy and had to be discarded. About half of the remaining trajectories did not react within 400 fs. A number of these initially unreactive trajectories were integrated for an additional 800 fs and showed roughly the same branching ratio.

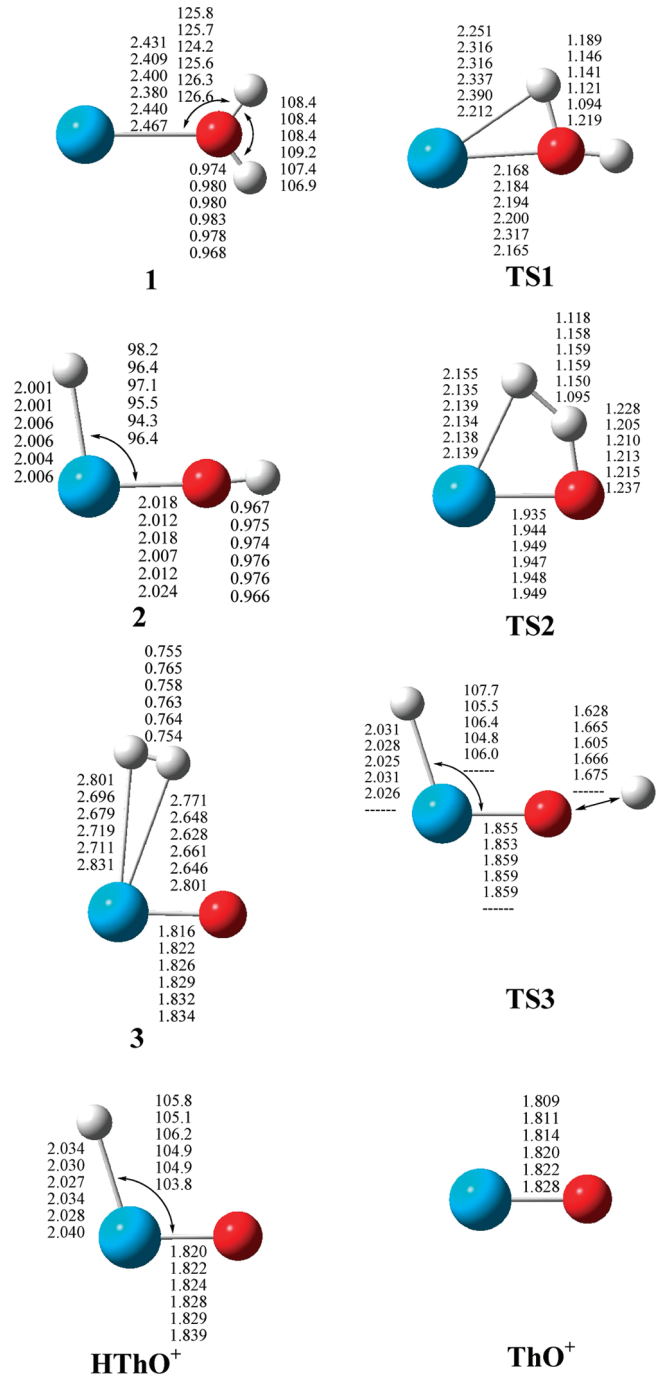

Figure 1. Structures and selected geometric parameters of stationary points on the $ThOH_2^+$ potential energy surface optimized at the B3LYP/SDD, PW91/SDD, TPSS/SDD, PW91/ZORA-SR, PW91/ZORA-SO, and CCSD(T)/SDD levels of theory (from top to bottom rows, respectively). Bond distances are in Å, and angles are in degrees.

Results and Discussion

Structures and Energetics. The optimized geometries of the $ThOH_2^+$ and various intermediates, transition states (TS), and products are shown in Figure 1 for a number of levels of theory. The relative energies of these stationary structures at the PW91/SDD level of theory are summarized in Figure 2. The study by Russo and co-workers[21] has shown that for the reaction of Th^+ with water, the reaction path evolves along the doublet surface from the formation of the initial Th^+-OH_2 complex to the $HThO^+ + H$ and $ThO^+ + H_2$ products. The present calculations confirm that the doublet transition state, **TS1**, is lower than the quartet **TS1′**. Although the doublet Th^+-OH_2 complex shows extensive spin contamination, the doublet transition state **TS1** has much less spin contamination and the quartet **TS1′** has even less (see Table 1). Spin projection would result in further lowering of the doublet **TS1** relative to the quartet. Beyond the transition state, the doublet surface is much lower in energy than the quartet spin surface (see Figure 2 and ref 21) and has very little spin contamination. Thus, we will focus our study on the doublet spin surface, and start at the doublet Th^+-OH_2 transition state. In addition to the B3LYP/SDD and PW91/ZORA-SR levels of theory used in the study by Russo and co-workers,[21] we also investigated the potential energy surface at several other levels of theory, including the PW91/SDD, TPSS/

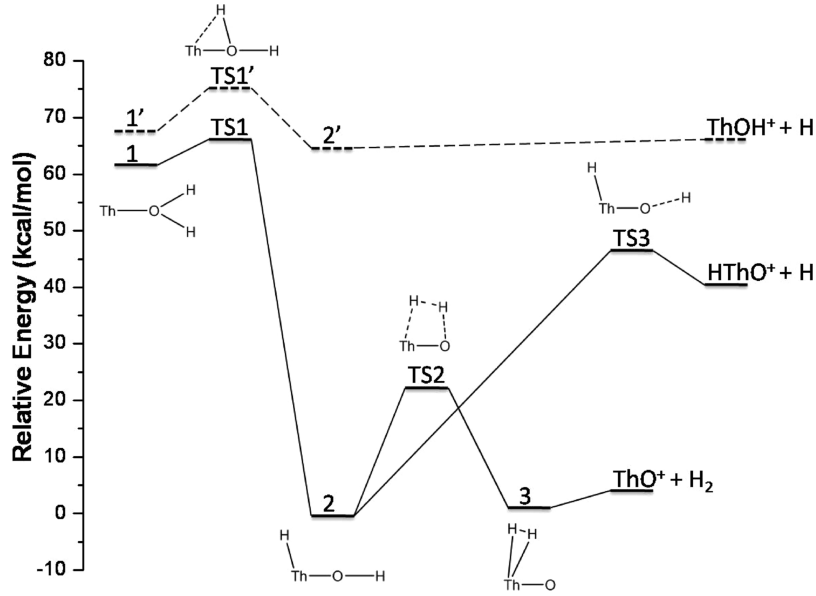

Figure 2. Potential energy profile for the isomerization and dissociation of $ThOH_2^+$ computed at the PW91/SDD level of theory.

TABLE 1: Relative Energies (kcal/mol) of the Various Points on the Doublet ThH_2O^+ Potential Energy Surface

	1	TS1	2	TS2	3	TS3	$ThO^+ + H_2$	$HThO^+ + H$
B3LYP[a]	61.8	69.4	0.0	29.1	3.2	54.9	3.9	46.1
PW91[a]	62.3	66.4	0.0	21.6	0.3	47.1	3.2	40.1
TPSS[a]	73.1	72.5	0.0	23.3	−0.8	46.2	2.6	40.4
BMK[a]	50.1	61.1	0.0	29.7	−4.5	51.4	−4.9	36.4
BH&HLYP[a]	52.9	64.3	0.0	32.8	−1.6	54.5	−0.8	40.6
PW91[b]	67.6	68.3	0.0	12.8	−19.5	40.1	−11.7	33.6
PW91[c]	69.8	69.0	0.0	19.6	−0.7	46.0	2.9	38.8
PW91[d]	66.1	68.1	0.0	19.8	0.0	46.5	4.0	39.6
CCSD(T)[a]	49.3	67.3	0.0	29.7	2.0	*f*	2.9	46.4
CCSD(T)[e]	60.4	72.4	0.0	29.7	0.4	*f*	2.3	44.5
$\langle S^2\rangle$[g]	1.3714	0.9457	0.7517	0.7516	0.7516	0.7588	0.7511	
PW91[h]	67.0	75.3	64.7					65.3
$\langle S^2\rangle$[i]	3.7525	3.7524	3.7527					2.0028 + 0.75

[a] SDD for Th and 6-311++G(d,p) for H and O atoms. [b] Frozen core TZP for Th and TZ2P for H and O atoms. [c] Frozen core TZP for Th and TZ2P for H and O atoms, ZORA-SR results. [d] Frozen core TZP for Th and TZ2P for H and O atoms, ZORA-SO results. [e] Estimated CCSD(T)/SDD+ energies using eq 1. [f] Cannot be located; the bond dissociation appears to proceed without a reverse barrier. [g] Expectation value of S^2 for the doublet surface at the PW91/SDD level of theory. [h] Quartet surface at the PW91/SDD level of theory. [i] Expectation value of S^2 for the quartet surface at the PW91/SDD level of theory.

SDD, PW91/ZORA-SO, CCSD(T)/SDD and est.CCSD(T)/SDD+ to assess the quality of these results (Table 1). These calculations cover pure GGA functionals, meta-GGAs, GGA with spin−orbit effect, and couple-cluster calculations with effective core potentials (ECP). This range of methods should provide a broad survey of the structures and energetics associated with the dissociation reaction of $ThOH_2^+$.

The calculations by Russo and co-workers[21] have shown that $ThOH_2^+$, **1**, is in a deep potential minimum, ca. 30 kcal/mol below reactants. At all levels of theory, they find Th^+ and H_2O form a strong bond, with R(Th−O) around 2.4 Å. The reaction proceeds through **TS1**, which is 4.1 kcal/mol higher than $ThOH_2^+$ at the PW91/SDD level. In **TS1**, one of the two H atoms migrates from O to Th, leading to $HThOH^+$, **2**. For the H_2 molecular elimination channel calculated at the PW91/SDD level, a barrier of 21.6 kcal/mol needs to be overcome first to reach H_2ThO^+, **3**, and then the H_2 molecule dissociates. For the H atom elimination channel, the barrier to break the O−H bond is much higher, 47.1 kcal/mol at the PW91/SDD level. This transition state, **TS3**, cannot be located by CCSD(T)/SDD, suggesting that there is no reverse barrier for the O−H bond dissociation at this level of theory.

The relative energies of selected stationary points on the potential energy surface have been computed at a number of levels of theory and are compared in Table 1. It is well-known that some DFT methods perform well in predicting energies, but the results can be sensitive to the functional. Therefore, a variety of DFT functionals have been employed to investigate the potential energy surface. Except for **1** and **TS1**, spin contamination is minimal. For the CCSD(T) calculation, the T1 diagnostic values for all the species are within the trust range,[45,46] less than 0.023, indicating single reference coupled cluster calculations should provide good results. The two methods that ought to be most reliable are PW91/ZORA-SO and est. CCSD(T)/SDD+. The latter uses a composite approach similar to G2(MP2) and G3(MP2) which are often employed in benchmark calculations. Spin−orbit effects are important in actinide compounds, and ZORA-SO calculations are an efficient way to take this into account. The est.CCSD(T)/SDD+ energies generally agree well with PW91/ZORA-SO with only one exception, **TS2**, which differs by approximately 10 kcal/mol. B3LYP/SDD agrees well with est.CCSD(T)/SDD+. BMK/SDD and BHandHLYP/SDD provide results that are similar to each other, but when compared to est.CCSD(T)/SDD+ both under-

TABLE 2: Vibrational Frequencies (cm^{-1}) of the Stationary Points at the PW91/SDD Level[a]

1	TS1	2	TS2	3	TS3	$HThO^+$
326.1	939.7*i*	319.4	1296.4*i*	163.7	1275.8*i*	366.2
370.2	322.4	471.0	804.2	344.6	211.5	910.4
458.0	531.7	484.5	1024.3	419.5	264.1	1598.5
1577.0	984.0	700.2	1145.0	689.4	349.5	
3572.3	1597.5	1629.1	1489.2	902.5	814.6	
3658.9	3662.5	3723.1	1880.9	4113.9	1596.1	

[a] ThO^+ 930.7; H_2 4330.0.

estimate all the relative energies except for **TS2**. TPSS/SDD shows better agreement in the dissociation energies of two products but gives a higher relative energy for $ThOH_2^+$, **1**. PW91/SDD is generally an improvement over TPSS/SDD. For PW91 with the frozen core TZ2P basis set, the ZORA-SR and ZORA-SO calculations agree well with each other (MAD less than 1.0 kcal/mol). Without ZORA-SR or ZORA-SO, some of the relative energies decrease by 5−20 kcal/mol. The PW91/SDD calculations are in good agreement with PW91/ ZORA-SO (MAD 1.2 kcal/mol) and CCSD(T)/SDD+ (MAD 3.1 kcal/mol). Therefore, PW91/SDD has been chosen for the trajectory calculations as a satisfactory yet practical compromise between the most trusted results.

The optimized geometries for the various stationary points are compared in Figure 1 and show relatively little dependence on the level of theory. For the minima, most bond lengths agree to within 0.01 Å and angles agree to ±1°. One exception is the Th−O bond length in complex **1**. Among the transition states, **TS1** shows some dependence on the level of theory, with the CCSD(T)/SDD calculations yielding a structure that is a bit later along the path toward $HThOH^+$. The transition state for H atom loss, **TS3**, could not be located at the CCSD(T)/SDD level, suggesting that O−H dissociation in $HThOH^+$ occurs without a reverse barrier. The vibrational frequencies for the stationary points calculated at the PW91/SDD level are listed in Table 2. Similar values are obtained with other levels of theory (see the Supporting Information).

Dynamics. The formation of the initial $Th-OH_2^+$ complex is quite exothermic, and a conservative estimate is that **TS1** lies at least 20 kcal/mol below the reactants, $Th^+ + H_2O$.[21] Since an additional 66.4 kcal/mol is released in the formation of the $HThOH^+$ intermediate from **TS1**, at least 86.4 kcal/mol is available for the dissociation of the $HThOH^+$. The branching ratio for the $ThO^+ + H_2$ and $HThO^+ + H$ products can be estimated by RRKM theory.[47,48] Using the vibrational data in Table 2 and an initial energy of 86.4 kcal/mol, a branching ratio of 8:1 is calculated in favor of $HThO^+ + H$. At first this may seem at odds with the energetics in Figure 2, since the barrier for the $HThO^+ + H$ channel is about twice as high as the barrier for the $ThO^+ + H_2$ channel. However, **TS3** has three low frequency vibrations whereas **TS2** has none, resulting in a much higher density of states at the available energy. The branching ratio predicted by RRKM is contrary to the observed branching ratio, which favors $ThO^+ + H_2$. With the large excess energy and the small number of vibrational modes, the reaction may occur more rapidly than the energy redistribution, and a statistical treatment may no longer be valid.

To obtain a better description of the branching ratio, the molecular dynamics of the $Th^+ + H_2O$ reaction were simulated using ab initio classical trajectory calculations. The foregoing discussion of the energetics showed that the PW91/SDD level of theory is suitable and practical for simulating the molecular dynamics (MD) of the $ThOH_2^+$ dissociation. Because the $Th^+ + H_2O$ reactants are at least 20 kcal/mol above **TS1**, the trajectories were started at the **TS1** with 20 kcal/mol extra energy distributed microcanonically among the vibration modes along with the transition vector. A total of 164 trajectories were integrated for up to 400 fs. The H_2 molecular elimination channel is dominant with a branching ratio of 41.5% compared to 6.7% for the H atom elimination channel. However, 51.8% trajectories do not dissociate in a simulation time of ca. 400 fs and stay in isomer **2**. Isomer **2** is a deep well on the potential energy surface, and longer simulation times are needed for these trajectories to dissociate. We chose 16 of these unreactive trajectories and integrated them for an additional 800 fs; 11 produced $ThO^+ + H_2$, 4 yielded $HThO^+ + H$, and 1 still did not dissociate. If the remaining trajectories dissociate with a similar ratio, the average branching ratio is ca. 80% for $ThO^+ + H_2$ and ca. 20% for $HThO^+ + H$.

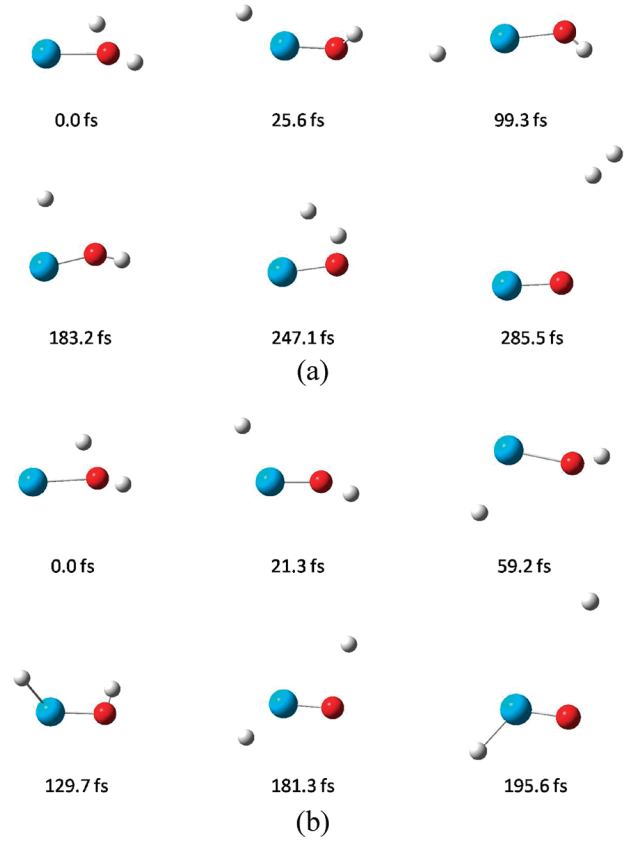

Figure 3. Snapshots of typical trajectories from the MD simulations: (a) $ThOH_2^+ \rightarrow ThO^+ + H_2$; (b) $ThOH_2^+ \rightarrow HThO^+ + H$. (The corresponding movies are available in the Supporting Information).

Two representative snapshots for H_2 molecular and H atomic elimination processes are shown in Figure 3 (the corresponding movies are available in the Supporting Information). The time to reach isomer **2** from **TS1** is relatively short, but dissociation of isomer **2** takes a longer time because it is in a fairly deep well. Both of the dissociation channels are exothermic compared to $Th^+ + H_2O$, but **TS3** lies considerably higher in energy than **TS2**. Insertion of Th^+ into H_2O to form $HThOH^+$ does not directly activate the OH bond that dissociates to form $HThO^+ + H$. However, the H bending modes are activated by the insertion, facilitating the two H atoms to come together to form an H−H bond.

Conclusions

The energetics of dissociation have been studied by a number of DFT and CCSD(T) levels of theory. Although the various

theoretical methods show some differences in the relative energies, the PW91/SDD level of theory provides a good compromise between accuracy and practicality. Both the H_2 molecular and H atom elimination channels are thermodynamically accessible, with a lower barrier for the former channel. The ab initio molecular dynamics study finds a branching ratio of ca. 80% for the H_2 molecular elimination reaction versus ca. 20% for the H atomic elimination reaction, compared with a branching ratio of 65% to 35%, respectively, observed in FTICR/MS experiments.

Acknowledgment. We thank Dr. Jason Sonnenberg (current address: Stevenson University) for advice and encouragement during the course of this work. This research was supported by grant from the National Science Foundation (CHE 0910858). Computer time made available by Supercomputer grid of Wayne State University and National Center for Supercomputing Applications is gratefully acknowledged.

Supporting Information Available: Vibrational frequencies of the stationary points at various levels of theory, movies of the trajectories in Figure 3, and the full citation for refs 30 and 35. This material is available free of charge via the Internet at http://pubs.acs.org.

References and Notes

(1) Gibson, J. K.; Haire, R. G.; Marçalo, J.; Santos, M.; Leal, J. P.; Pires de Matos, A.; Tyagi, R.; Mrozik, M. K.; Pitzer, R. M.; Bursten, B. E. *Eur. Phys. J. D* **2007**, *45*, 133–138.

(2) Gibson, J. K.; Marçalo, J. *Coord. Chem. Rev.* **2006**, *250*, 776–783.

(3) Gibson, J. K. *Int. J. Mass Spectrom.* **2002**, *214*, 1–21.

(4) Gibson, J. K.; Haire, R. G. *Inorg. Chem.* **2002**, *41*, 5897–5906.

(5) Gibson, J. K.; Haire, R. G. *Radiochim. Acta* **2003**, *91*, 441–448.

(6) Gibson, J. K.; Haire, R. G. *Organometallics* **2005**, *24*, 119–126.

(7) Santos, M.; Marçalo, J.; Leal, J. P.; Pires de Matos, A.; Gibson, J. K.; Haire, R. G. *Int. J. Mass Spectrom.* **2003**, *228*, 457–465.

(8) Santos, M.; Marçalo, J.; Pires de Matos, A.; Gibson, J. K.; Haire, R. G. *J. Phys. Chem. A* **2002**, *106*, 7190–7194.

(9) Cornehl, H. H.; Wesendrup, R.; Diefenbach, M.; Schwarz, H. *Chem.—Eur. J.* **1997**, *3*, 1083–1090.

(10) Gibson, J. K.; Haire, R. G.; Santos, M.; Marçalo, J.; Pires de Matos, A. *J. Phys. Chem. A* **2005**, *109*, 2768–2781.

(11) Gibson, J. K.; Haire, R. G.; Marçalo, J.; Santos, M.; Pires de Matos, A.; Mrozik, M. K.; Pitzer, R. M.; Bursten, B. E. *Organometallics* **2007**, *26*, 3947–3956.

(12) Heinemann, C.; Cornehl, H. H.; Schwarz, H. *J. Organomet. Chem.* **1995**, *501*, 201–209.

(13) Marçalo, J.; Leal, J. P.; Pires de Matos, A. *Int. J. Mass Spectrom.* **1996**, *157*, 265–274.

(14) Marçalo, J.; Leal, J. P.; Pires de Matos, A.; Marshall, A. G. *Organometallics* **1997**, *16*, 4581–4588.

(15) Jackson, G. P.; King, F. L.; Goeringer, D. E.; Duckworth, D. C. *J. Phys. Chem. A* **2002**, *106*, 7788–7794. *108*, 2139.

(16) Jackson, G. P.; Gibson, J. K.; Duckworth, D. C. *Int. J. Mass Spectrom.* **2002**, *220*, 419–441.

(17) Jackson, G. P.; Gibson, J. K.; Duckworth, D. C. *J. Phys. Chem. A* **2004**, *108*, 1042–1051.

(18) Michelini, M. C.; Russo, N.; Sicilia, E. *Angew. Chem., Int. Ed.* **2006**, *45*, 1095–1099.

(19) Michelini, M. C.; Russo, N.; Sicilia, E. *J. Am. Chem. Soc.* **2007**, *129*, 4229–4239.

(20) Alikhani, M. E.; Michelini, M. C.; Russo, N.; Silvi, B. *J. Phys. Chem. A* **2008**, *112*, 12966–12974.

(21) Mazzone, G.; Michelini, M. C.; Russo, N.; Sicilia, E. *Inorg. Chem.* **2008**, *47*, 2083–2088.

(22) Becke, A. D. *J. Chem. Phys.* **1993**, *98*, 1372–1377.

(23) Becke, A. D. *J. Chem. Phys.* **1993**, *98*, 5648–5652.

(24) Lee, C.; Yang, W.; Parr, R. G. *Phys. Rev. B* **1988**, *37*, 785.

(25) Perdew, J. P.; Chevary, J. A.; Vosko, S. H.; Jackson, K. A.; Pederson, M. R.; Singh, D. J.; Fiolhais, C. *Phys. Rev. B* **1992**, *46*, 6671–6687.

(26) Perdew, J. P.; Burke, K.; Wang, Y. *Phys. Rev. B* **1996**, *54*, 16533–16539.

(27) Tao, J.; Perdew, J. P.; Staroverov, V. N.; Scuseria, G. E. *Phys. Rev. Lett.* **2003**, *91*, 146401.

(28) Boese, A. D.; Jan, M. L. M. *J. Chem. Phys.* **2004**, *121*, 3405–3416.

(29) Kuchle, W.; Dolg, M.; Stoll, H.; Preuss, H. *J. Chem. Phys.* **1994**, *100*, 7535–7542.

(30) Frisch, M. J.; Trucks, G. W.; Schlegel, H. B.; et al. *Gaussian DV*, revision F.02; Gaussian, Inc.: Wallingford, CT, 2007.

(31) Velde, G. T.; Bickelhaupt, F. M.; Baerends, E. J.; Guerra, C. F.; Van Gisbergen, S. J. A.; Snijders, J. G.; Ziegler, T. *J. Comput. Chem.* **2001**, *22*, 931–967.

(32) Guerra, C. F.; Snijders, J. G.; te Velde, G.; Baerends, E. J. *Theor. Chem. Acc.* **1998**, *99*, 391–403.

(33) ADF; ADF 2007.01 ed.; SCM, Theoretical Chemistry, Vrije Universiteit: Amsterdam, The Netherlands, http://www.scm.com.

(34) Pople, J. A.; Head-Gordon, M.; Raghavachari, K. *J. Chem. Phys.* **1987**, *87*, 5968–5975.

(35) Werner, H.-J.; Knowles, P. J.; Lindh, R.; et al. MOLPRO version 2006.1. A package of ab initio programs.

(36) Curtiss, L. A.; Raghavachari, K.; Pople, J. A. *J. Chem. Phys.* **1993**, *98*, 1293–1298.

(37) Curtiss, L. A.; Redfern, P. C.; Raghavachari, K.; Rassolov, V.; Pople, J. A. *J. Chem. Phys.* **1999**, *110*, 4703–4709.

(38) Bakken, V.; Millam, J. M.; Schlegel, H. B. *J. Chem. Phys.* **1999**, *111*, 8773–8777.

(39) Millam, J. M.; Bakken, V.; Chen, W.; Hase, W. L.; Schlegel, H. B. *J. Chem. Phys.* **1999**, *111*, 3800–3805.

(40) Stoer, J.; Bulirsch, R. *Introduction to Numerical Analysis*; Springer-Verlag: New York, 1980.

(41) Hase, W. L. Classical Trajectory Simulations: Initial Conditions. In *Encyclopedia of Computational Chemistry*; Schleyer, P. v. R., Allinger, N. L., Clark, T., Gasteiger, J., Kollman, P. A., Schaefer III, H. F., Schreiner, P. R., Eds.; Wiley: Chichester, U.K., 1998; pp 402−407.

(42) Peslherbe, G. H.; Wang, H.; Hase, W. L. *Adv. Chem. Phys.* **1999**, *105*, 171–201.

(43) Anand, S.; Schlegel, H. B. *Phys. Chem. Chem. Phys.* **2004**, *6*, 5166–5171.

(44) Zhou, J.; Schlegel, H. B. *J. Phys. Chem. A* **2008**, *112*, 13121–13127.

(45) Lee, T. J.; Taylor, P. R. *Int. J. Quantum Chem.* **1989**, 199–207.

(46) Rienstra-Kiracofe, J. C.; Allen, W. D.; Schaefer, H. F. *J. Phys. Chem. A* **2000**, *104*, 9823–9840.

(47) Marcus, R. A.; Rice, O. K. *J. Phys. Chem.* **1951**, *55*, 894–908.

(48) Steinfeld, J. I.; Francisco, J. S.; Hase, W. L. *Chemical Kinetics and Dynamics*, 2nd ed.; Prentice Hall: Upper Saddle River, NJ, 1999.

JP912098W